

Emergence of near-threshold structures in heavy hadron spectrum

郭奉坤

中国科学院理论物理研究所

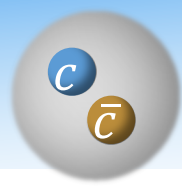
General model-independent analysis on threshold structures:

X.-K. Dong, FKG, B.-S. Zou, Phys. Rev. Lett. 126 (2021) 152001 [arXiv:2011.14517]

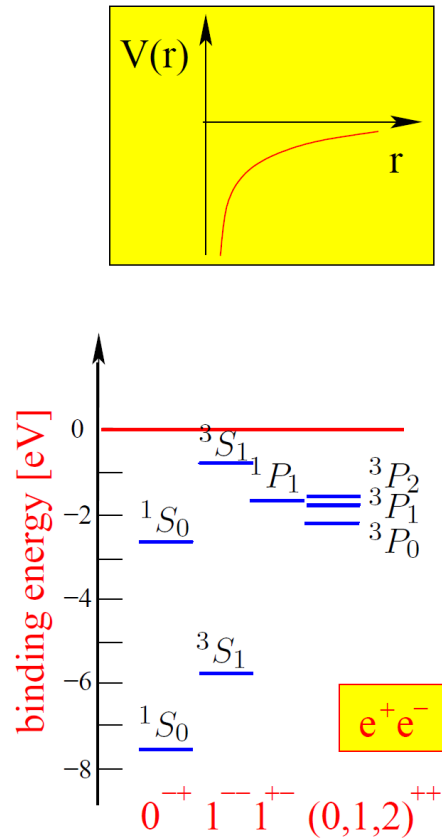
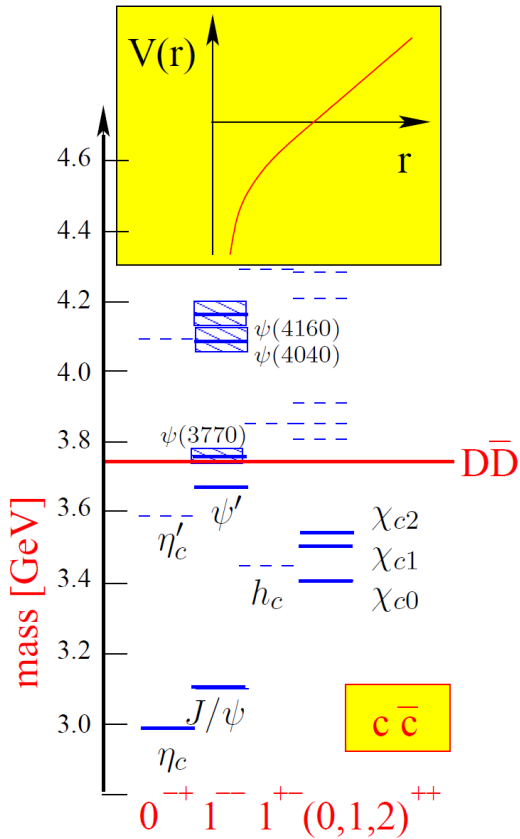
Systematic spectrum of hadronic molecules:

X.-K. Dong, FKG, B.-S. Zou, 《物理学进展》 41 (2021) 65 [arXiv:2101.01021]; Commun. Theor. Phys. 73 (2021) 125201 [arXiv:2108.02673]

Charmonium

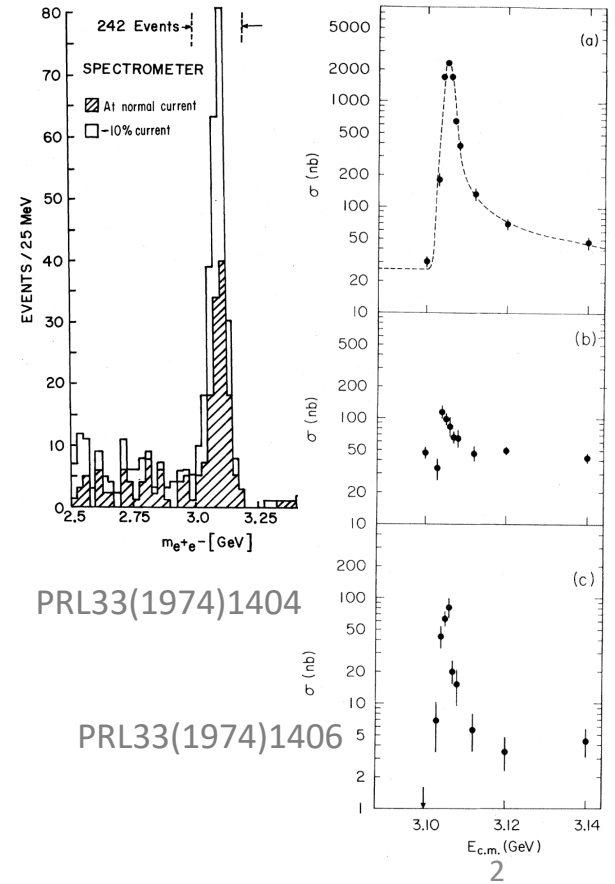


- Meson consisting of a charm quark and an anticharm quark
 - The first charmonium: J/ψ
 - Probing both perturbative and nonperturbative QCD



From talk by Hanhart at APS2018

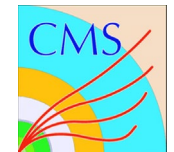
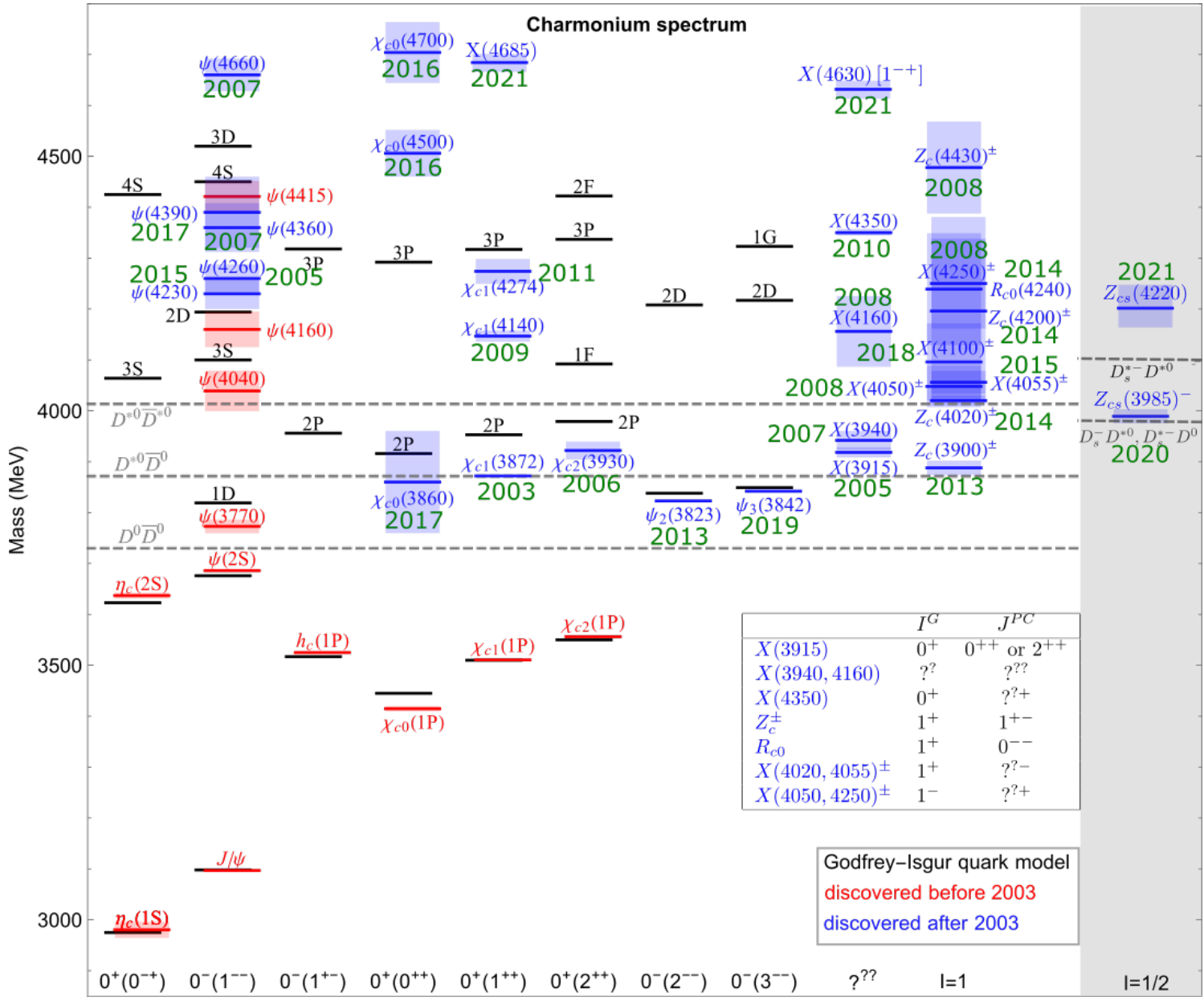
Cornell potential model:
Eichten et al., PRD17(1978)3090



PRL33(1974)1404

PRL33(1974)1406

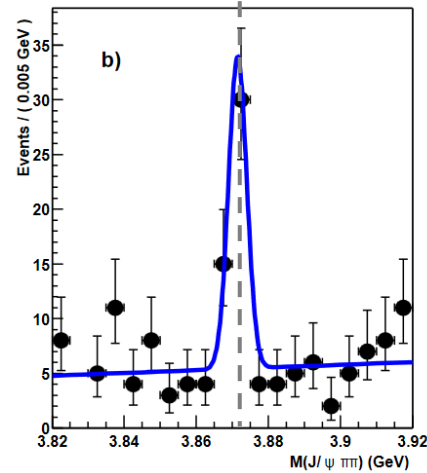
Charmonium(-like) structures



Charmonium-like structures

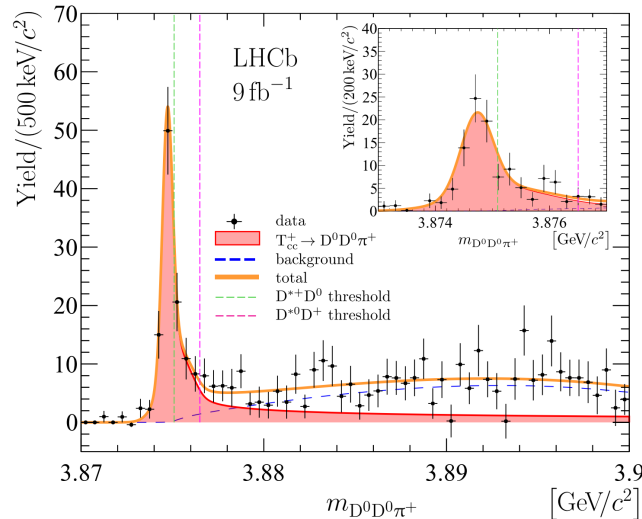
- X(3872) Belle, PRL91(2003)262001

$D^0 \bar{D}^{*0}$ thr.



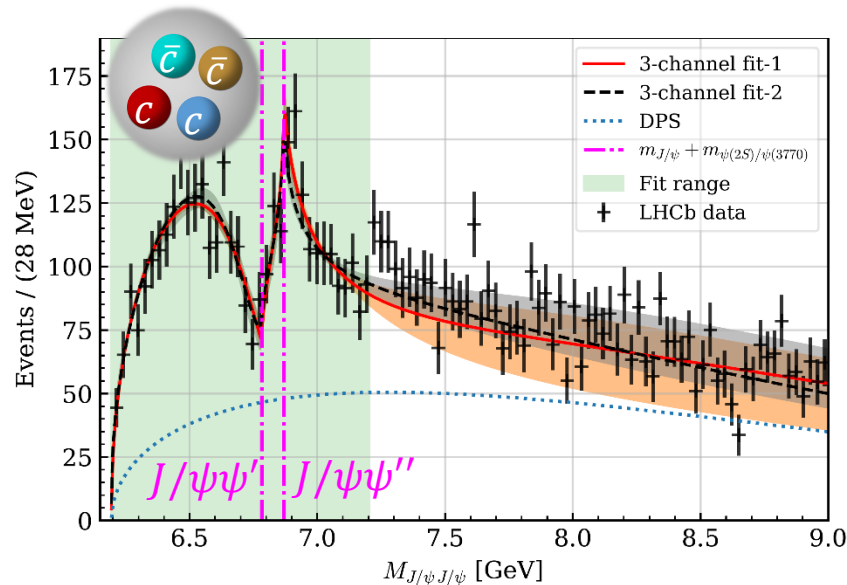
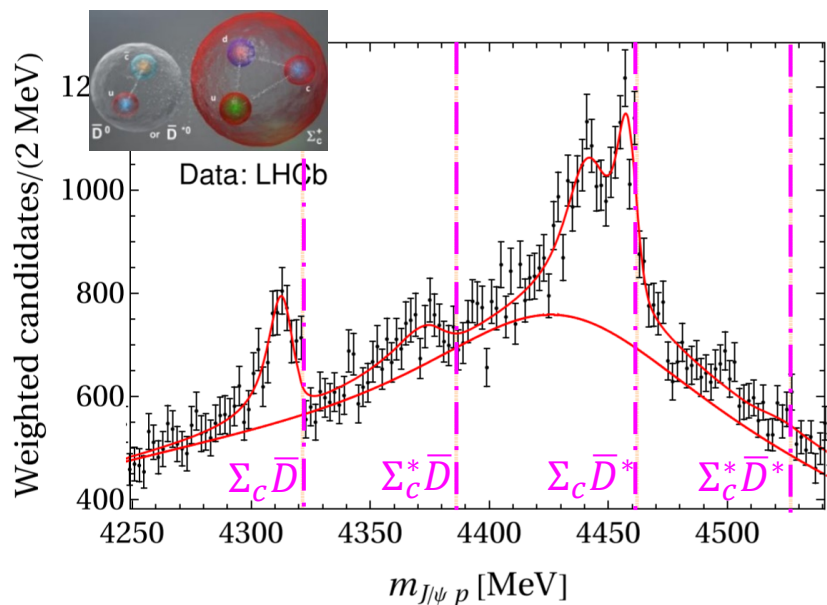
- T_{cc}^+

$D^0 D^{*+}$ thr.



LHCb, arXiv:2109.01038; arXiv:2109.01056

P_c and double- J/ψ structures



data from LHCb, PRL122 (2019) 222001;
 fit from
 M.-L. Du, Baru, FKG, Hanhart, Meißner, Oller, Q. Wang,
 PRL124 (2020) 072001

data from LHCb, Sci.Bull.65 (2020) 1983;
 fit from
 X.-K. Dong, Baru, FKG, Hanhart, Nedefiev,
 PRL126 (2021) 132001

Many new structures are near thresholds of a pair of heavy hadrons.

Why are there so many (near-)threshold structures in heavy-hadron spectrum?

Is there any rule?

Effective range expansion

$$f_0^{-1}(k) = \frac{1}{a_0} + \frac{1}{2}r_0k^2 - ik + \mathcal{O}\left(\frac{k^4}{\beta^4}\right)$$

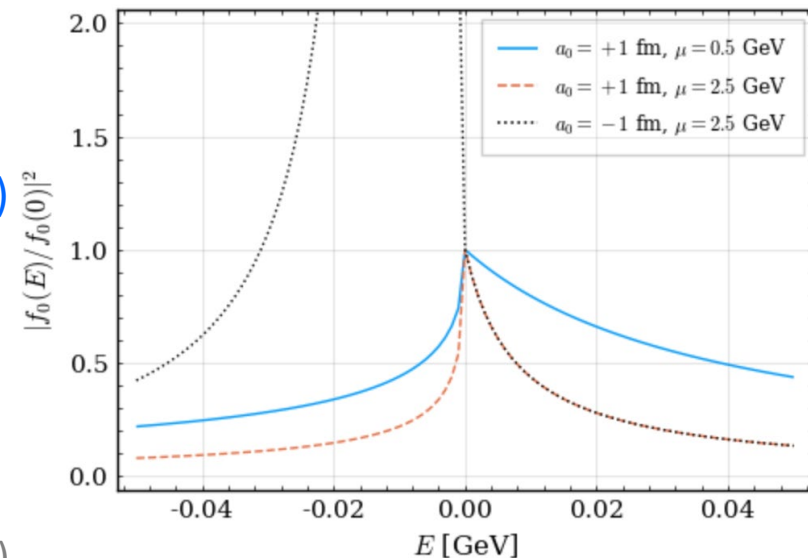
a_0 : S-wave scattering length; **negative for repulsion or attraction w/ a bound state**
positive for attraction w/o bound state

Very close to threshold, then scattering length approximation: $f_0^{-1}(E) = \frac{1}{a_0} - i\sqrt{2\mu E}$.

$$|f_0(E)|^2 = \begin{cases} \frac{1}{1/a_0^2 + 2\mu E} & \text{for } E \geq 0 \\ \frac{1}{(1/a_0 + \sqrt{-2\mu E})^2} & \text{for } E < 0 \end{cases}$$

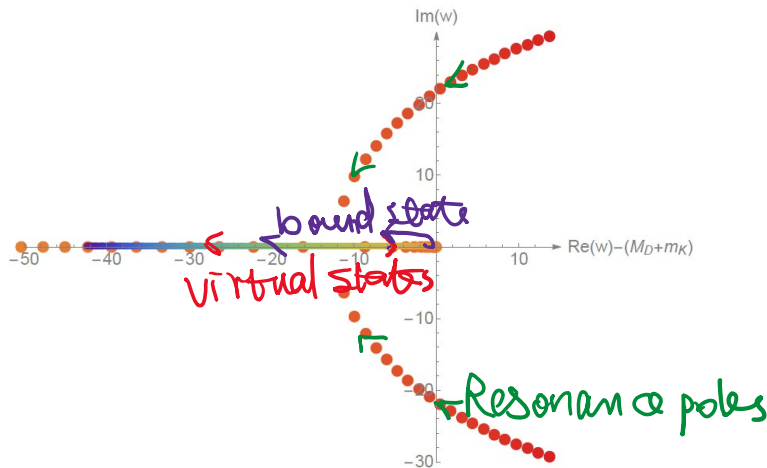
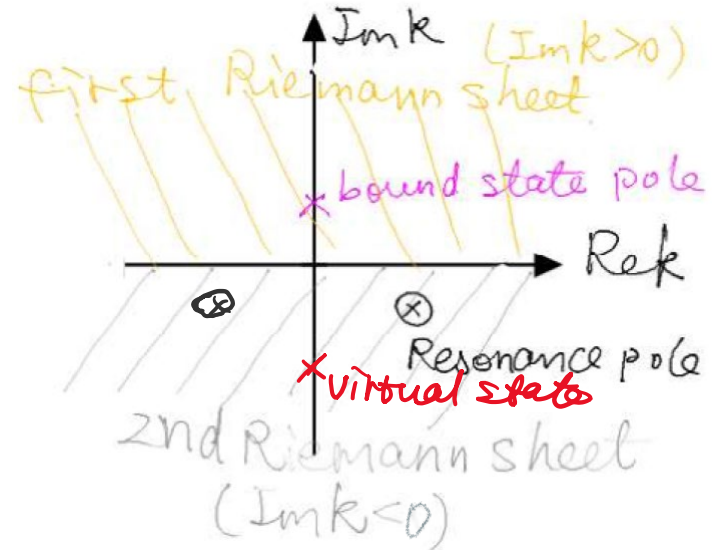
- Cusp at threshold ($E=0$)
- Maximal at threshold for **positive a_0 (attraction)**
- Half-maximum width: $\frac{2}{\mu a_0^2}$;
virtual state pole at $E_{\text{virtual}} = -1/(2\mu a_0^2)$
- Strong interaction, a_0 becomes negative, **pole below threshold**, peak below threshold

see also, e.g., Brambilla et al. Phys. Rept. 873, 1 (2020)



Bound state, virtual state and resonance

- **Bound state**: pole below threshold on real axis of the first Riemann sheet of complex energy plane
- **Virtual state**: pole below threshold on real axis of the second Riemann sheet
- **Resonance**: pole in the complex plane on the second Riemann sheet

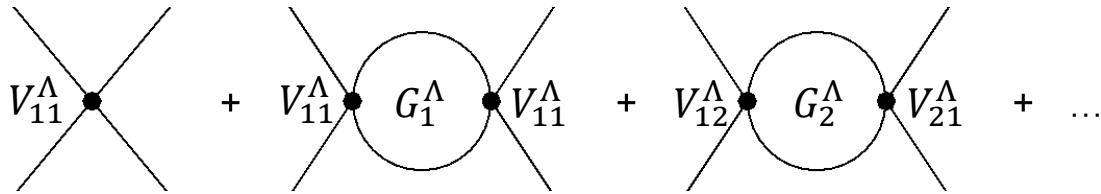


Plot from Matuschek, Baru, FKG, Hanhart, EPJA57(2021)101

For $\frac{1}{1/a_0 - i k}$, only bound or virtual state poles are possible

Coupled channels

- Full threshold structure needs to be measured in a lower channel \Rightarrow coupled channels
- Consider a two-channel system, construct a nonrelativistic effective field theory (NREFT)
 - Energy region around the higher threshold, Σ_2
 - Expansion in powers of $E = \sqrt{s} - \Sigma_2$
 - Momentum in the lower channel can also be expanded



$$T(E) = V + VG(E)V + VG(E)VG(E)V + \dots = \frac{1}{V^{-1} - G(E)}$$

$$G_1^\Lambda(E) = i \int^{\Lambda_1} \frac{d^4q}{(2\pi)^2} \frac{1}{(q^2 - m_{1,1}^2 + i\epsilon)[(P - q)^2 - m_{1,2}^2 + i\epsilon]} = R(\Lambda_1) - i \frac{k_1}{8\pi\sqrt{s}}$$

$$G_2^\Lambda(E) = - \frac{1}{4m_{2,1}m_{2,2}} \int^{\Lambda_2} \frac{d^3\mathbf{q}}{(2\pi)^3} \frac{2\mu_2}{\mathbf{q}^2 - 2\mu_2 E - i\epsilon} = \frac{1}{8\pi\Sigma_2} \left[-\frac{2\Lambda_2}{\pi} + \boxed{\sqrt{-2\mu_2 E - i\epsilon}} + \mathcal{O}\left(\frac{k_2^2}{\Lambda_2}\right) \right]$$

- Λ dependence absorbed by V^{-1}

Nonanalyticity only from here



NREFT at LO

- Very close to the higher threshold, LO:

$$\begin{aligned}
 T(E) &= 8\pi\Sigma_2 \left(\begin{array}{cc} -\frac{1}{a_{11}} + ik_1 & \frac{1}{a_{12}} \\ \frac{1}{a_{12}} & -\frac{1}{a_{22}} - \sqrt{-2\mu_2 E - i\epsilon} \end{array} \right)^{-1} \\
 &= -\frac{8\pi\Sigma_2}{\det} \left(\begin{array}{cc} \frac{1}{a_{22}} + \sqrt{-2\mu_2 E - i\epsilon} & \frac{1}{a_{12}} \\ \frac{1}{a_{12}} & \frac{1}{a_{11}} - ik_1 \end{array} \right), \\
 \det &= \left(\frac{1}{a_{11}} - ik_1 \right) \left(\frac{1}{a_{22}} + \sqrt{-2\mu_2 E - i\epsilon} \right) - \frac{1}{a_{12}^2}
 \end{aligned}$$

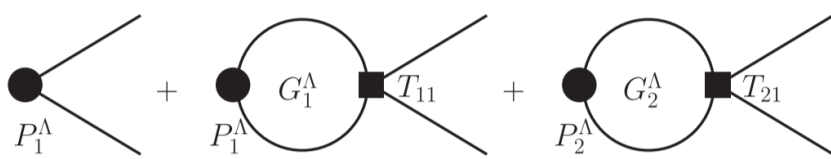
Effective scattering length with open-channel effects becomes **complex**, $\text{Im} \frac{1}{a_{22,\text{eff}}} \leq 0$

$$T_{22}(E) = -\frac{8\pi}{\Sigma_2} \left[\frac{1}{a_{22,\text{eff}}} - i\sqrt{2\mu_2 E} + \mathcal{O}(E) \right]^{-1}$$

$$\frac{1}{a_{22,\text{eff}}} = \frac{1}{a_{22}} - \frac{a_{11}}{a_{12}^2(1 + a_{11}^2 k_1^2)} - i \frac{a_{11}^2 k_1}{a_{12}^2(1 + a_{11}^2 k_1^2)}.$$

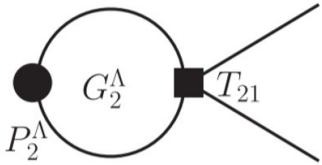
NREFT at LO

- Consider a production process, **must** go through final-state interaction (**unitarity**)



$$\begin{aligned}
 & P_1^\Lambda [1 + G_1^\Lambda T_{11}(E)] + P_2^\Lambda G_2^\Lambda(E) T_{21}(E) \\
 &= P_1^\Lambda (V_{11}^\Lambda)^{-1} T_{11}(E) + [P_1^\Lambda (V_{11}^\Lambda)^{-1} V_{12}^\Lambda + P_2^\Lambda] G_2^\Lambda T_{21}(E) \\
 &\equiv P_1 T_{11}(E) + P_2 T_{21}(E)
 \end{aligned}$$

- All nontrivial energy dependence are contained in $T_{11}(E)$ and $T_{21}(E)$
- Case-1: dominated by $T_{21}(E)$,

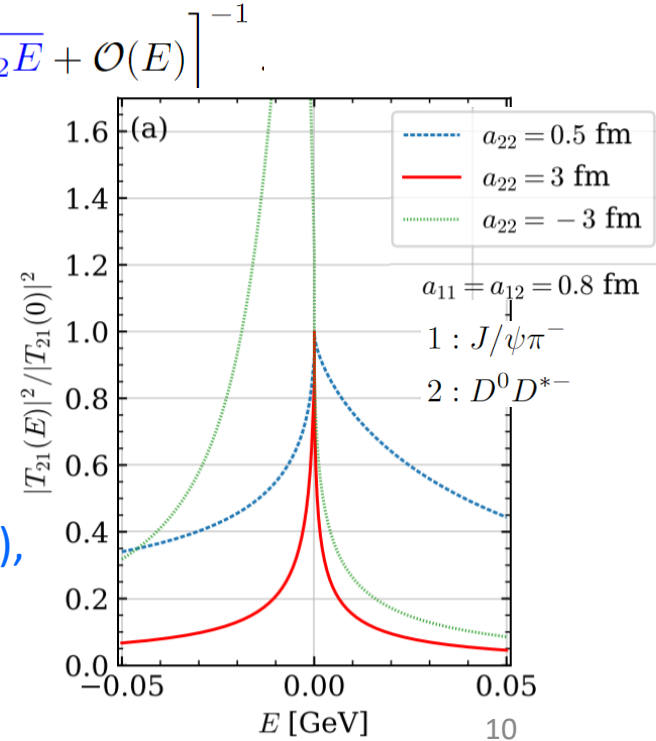


$$T_{21}(E) = \frac{-8\pi\Sigma_2}{a_{12}(1/a_{11} - ik_1)} \left[\frac{1}{a_{22,\text{eff}}} - i\sqrt{2\mu_2 E} + \mathcal{O}(E) \right]^{-1}$$

$$|T_{21}(E)|^2 \propto |T_{22}(E)|^2 \propto$$

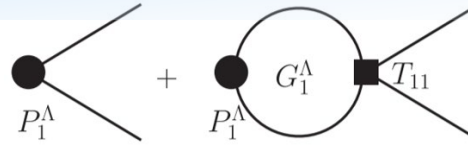
$$\begin{cases} \left[\left(\text{Re} \frac{1}{a_{22,\text{eff}}} \right)^2 + \left(\text{Im} \frac{1}{a_{22,\text{eff}}} - \sqrt{2\mu E} \right)^2 \right]^{-1} & \text{for } E \geq 0 \\ \left[\left(\text{Im} \frac{1}{a_{22,\text{eff}}} \right)^2 + \left(\text{Re} \frac{1}{a_{22,\text{eff}}} + \sqrt{-2\mu E} \right)^2 \right]^{-1} & \text{for } E < 0 \end{cases}$$

- Maximal at threshold for **positive** $\text{Re}(a_{22,\text{eff}})$ (attraction), $\text{FWHM} \propto 1/\mu$
- Peaking at pole for negative $\text{Re}(a_{22,\text{eff}})$



NREFT at LO

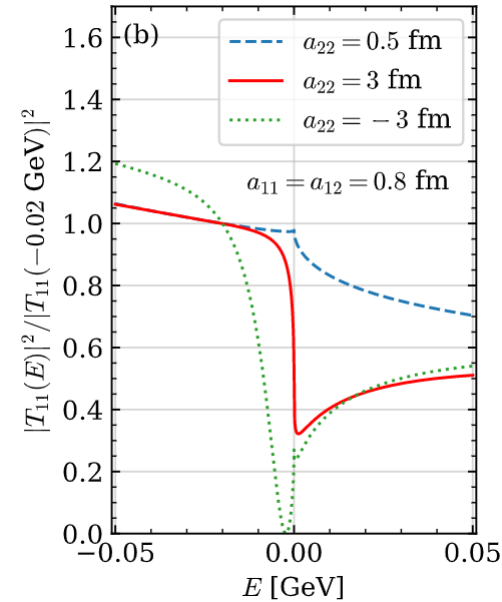
- Case-2: dominated by $T_{11}(E)$



$$T_{11}(E) = \frac{-8\pi\Sigma_2 \left(\frac{1}{a_{22}} - i\sqrt{2\mu_2 E} \right)}{\left(\frac{1}{a_{11}} - i k_1 \right) \left[\frac{1}{a_{22,\text{eff}}} - i\sqrt{2\mu_2 E} + \mathcal{O}(E) \right]}$$

- One pole and one zero
- For strongly interacting channel-2 (large a_{22}), there must be a dip around threshold (zero close to threshold)

$$\frac{1}{a_{22,\text{eff}}} = \frac{1}{a_{22}} - \frac{a_{11}}{a_{12}^2(1 + a_{11}^2 k_1^2)} - i \frac{a_{11}^2 k_1}{a_{12}^2(1 + a_{11}^2 k_1^2)}$$



Poles in complex momentum plane:

$$(0.37 - i0.08)\text{GeV}$$

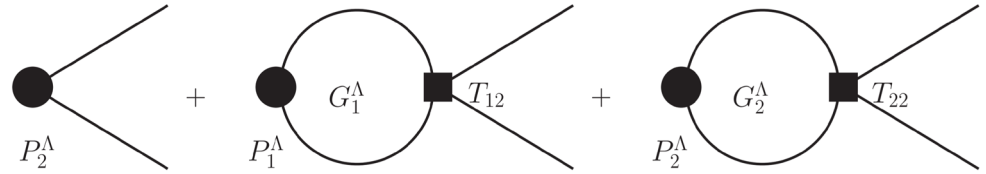
$$(0.04 - i0.08)\text{GeV}$$

$$(-0.09 - i0.08)\text{GeV}$$

- More complicated line shape if both channels are important for the production

NREFT at LO

- Case-3: final states in channel-2



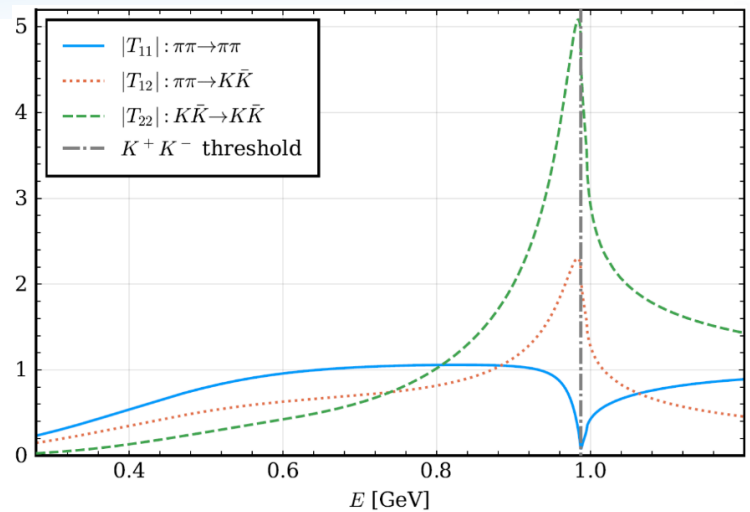
$$P_1 T_{12}(E) + P_2 T_{22}(E) \propto \left[\frac{1}{a_{22,\text{eff}}} - i\sqrt{2\mu_2 E} + \mathcal{O}(E) \right]^{-1}$$

- Suppression due to phase space
- Peak just above threshold would require the pole to be nearby

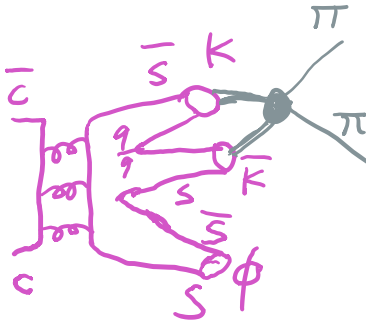
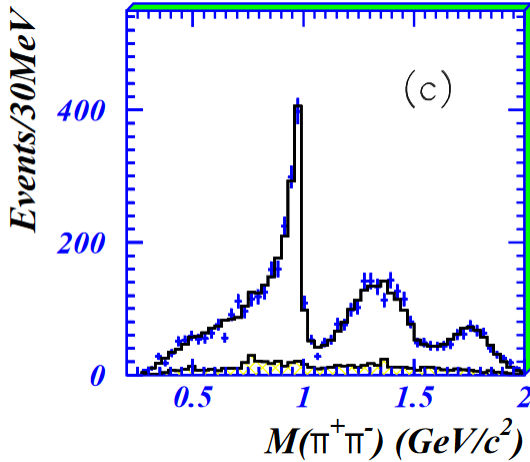
Phenomenology

- T -matrix for $\pi\pi$ and $K\bar{K}$ coupled channels

with the T-matrix from
L.-Y. Dai, M. R. Pennington, PRD90(2014)036004



- $f_0(980)$ in $J/\psi \rightarrow \phi\pi^+\pi^-$ and

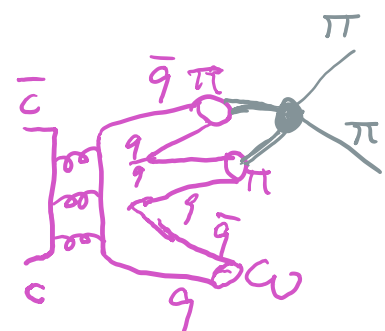
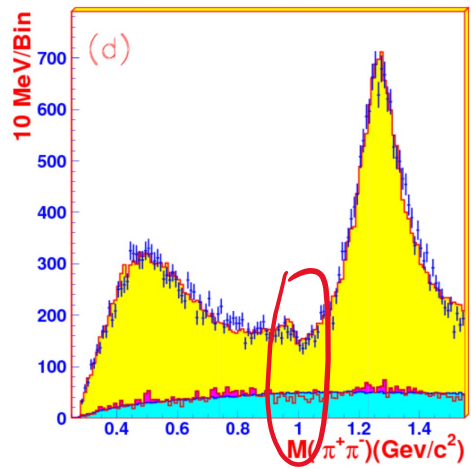


BES,
PLB607(2005)243

Driving channel: $K\bar{K}$

$$J/\psi \rightarrow \phi K\bar{K} \rightarrow \phi\pi^+\pi^-$$

- $J/\psi \rightarrow \omega\pi^+\pi^-$ Channels: $\pi\pi$ and $K\bar{K}$



BES,
PLB598(2004)149

Driving channel: $\pi\pi$

$$J/\psi \rightarrow \omega\pi\pi \rightarrow \omega\pi^+\pi^-$$



Phenomenology

- Production of states with hidden-charm and hidden-bottom: **open-flavor much easier than $Q\bar{Q} + \text{light hadrons}$** , generally peaks around threshold of a pair of open-flavor hadrons for **attractive interaction**
- Complications due to more channels
- Threshold structures should be **more pronounced in bottom-bottom and bottom-charm than in charm-charm**
 - **Either threshold cusp or below-threshold peak**
 - **peak width $\propto 1/m_Q$ for fixed a**
 - **Perturbative estimate of scattering length: $a \propto m_Q$ [potential independent of m_Q]; nonperturbative for strong attraction, **near-threshold pole****

Model estimate of near-th. interactions

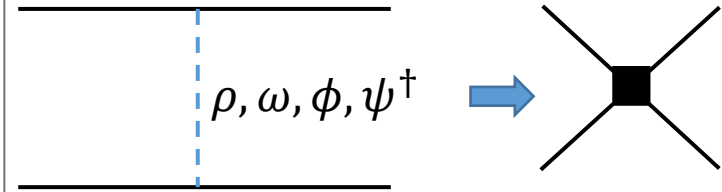
- Constant contact terms saturated by light-vector-meson exchange, similar to **VMD in the resonance saturation** of the low-energy constants in CHPT

V, A, S, S_1 and η_1 contributions to the coupling constants L_i^r in units of 10^{-3} .

	$L_i^r(M_\rho)$	V	A	S	S_1	η_1	Total
L_1^r	0.7 ± 0.3	0.6	0	-0.2	$0.2^{b)}$	0	0.6
L_2^r	1.3 ± 0.7	1.2	0	0	0	0	1.2
L_3^r	-4.4 ± 2.5	-3.6	0	0.6	0	0	-3.0
L_4^r	-0.3 ± 0.5	0	0	-0.5	$0.5^{b)}$	0	0.0
L_5^r	1.4 ± 0.5	0	0	$1.4^{a)}$	0	0	1.4
L_6^r	-0.2 ± 0.3	0	0	-0.3	$0.3^{b)}$	0	0.0
L_7^r	-0.4 ± 0.15	0	0	0	0	-0.3	-0.3
L_8^r	0.9 ± 0.3	0	0	$0.9^{a)}$	0	0	0.9
L_9^r	6.9 ± 0.7	$6.9^{a)}$	0	0	0	0	6.9
L_{10}^r	-5.2 ± 0.3	-10.0	4.0	0	0	0	-6.0

^{a)} Input.
^{b)} Large- N_C estimate.

Ecker, Gasser, Pich, de Rafael, NPB321(1989)311



- List of attractive pairs of charm-anticharm hadron pairs

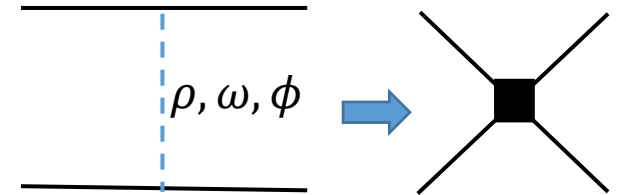
$H\bar{H}$	$D^{(*)}\bar{D}^{(*)}[0, 1^\dagger];$ $X(3872), Z_c(3900, 4020)$ $Z_b(10610, 10650)$	$D_s^{(*)}\bar{D}^{(*)}[\frac{1}{2}^\dagger];$ $Z_{cs}(3985)$	$D_s^{(*)}\bar{D}_s^{(*)}[0]$ $X(4140)$
$\bar{H}T$	$\bar{D}^{(*)}\Xi_c[0];$ $P_{cs}(4459)$	$\bar{D}_s^{(*)}\Lambda_c[0^\dagger]$	
$\bar{H}S$	$\bar{D}^{(*)}\Sigma_c^{(*)}[\frac{1}{2}];$ $P_c(4312, 4440, 4457)$ $\bar{D}^{(*)}\Omega_c^{(*)}[\frac{1}{2}^\dagger]$	$\bar{D}_s^{(*)}\Sigma_c^{(*)}[1^\dagger];$	$\bar{D}^{(*)}\Xi_c^{\prime(*)}[0];$
$T\bar{T}$	$\Lambda_c\bar{\Lambda}_c[0];$	$\Lambda_c\bar{\Xi}_c[\frac{1}{2}];$	$\Xi_c\bar{\Xi}_c[0, 1]$
$T\bar{S}$	$\Lambda_c\bar{\Sigma}_c^{(*)}[1];$ $\Xi_c\bar{\Sigma}_c^{(*)}[\frac{3}{2}^\dagger, \frac{1}{2}];$	$\Lambda_c\bar{\Xi}_c^{\prime(*)}[\frac{1}{2}];$ $\Xi_c\bar{\Xi}_c^{\prime(*)}[1, 0];$	$\Lambda_c\bar{\Omega}_c^{(*)}[0^\dagger];$ $\Xi_c\bar{\Omega}_c^{(*)}[\frac{1}{2}];$
$S\bar{S}$	$\Sigma_c^{(*)}\bar{\Sigma}_c^{(*)}[2^\dagger, 1, 0];$ $\Xi_c^{\prime(*)}\bar{\Xi}_c^{\prime(*)}[1, 0];$	$\Sigma_c^{(*)}\bar{\Xi}_c^{\prime(*)}[\frac{3}{2}^\dagger, \frac{1}{2}];$ $\Xi_c^{\prime(*)}\bar{\Omega}_c^{(*)}[\frac{1}{2}];$	$\Sigma_c^{(*)}\bar{\Omega}_c^{(*)}[0^\dagger];$ $\Omega_c^{(*)}\bar{\Omega}_c^{(*)}[0]$

Hadronic molecules from VMD interactions

- Approximations:

- Constant contact terms (V) saturated by light-vector-meson exchange, similar to the **vector-meson dominance in the resonance saturation** of the low-energy constants in CHPT
- Single channels
- Neglecting mixing with normal charmonia

G. Ecker, J. Gasser, A. Pich, E. de Rafael, NPB321(1989)311

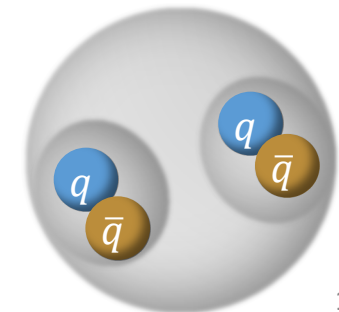


- The T-matrix:

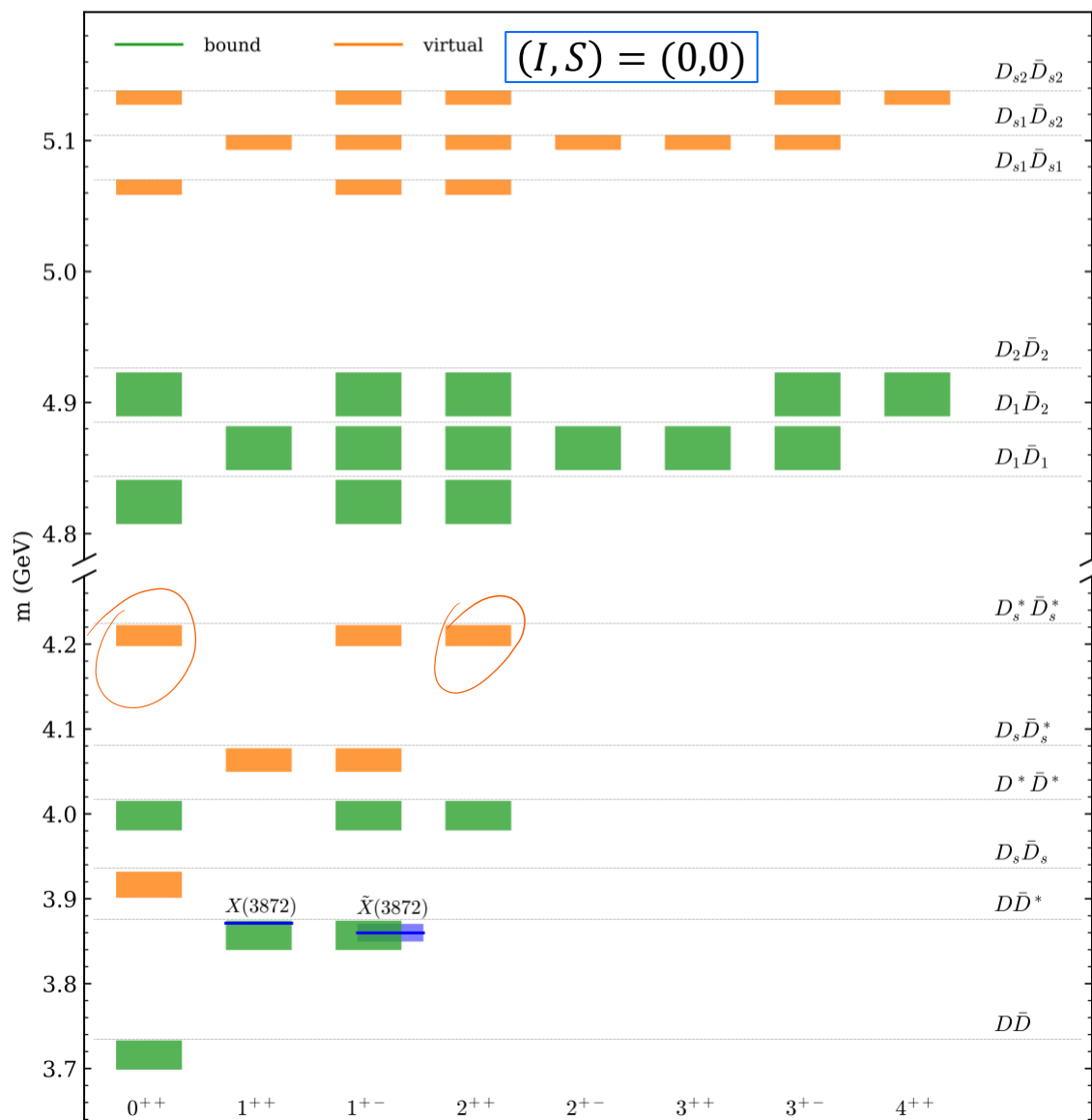
$$T = \frac{V}{1 - VG}$$

G : two-point scalar loop integral regularized using dim.reg. with a subtraction constant matched to a Gaussian regularized G at threshold, with cutoff $\Lambda \in [0.5, 1.0]$ GeV

- Hadronic molecules appear as **bound or virtual state poles** of the T matrix

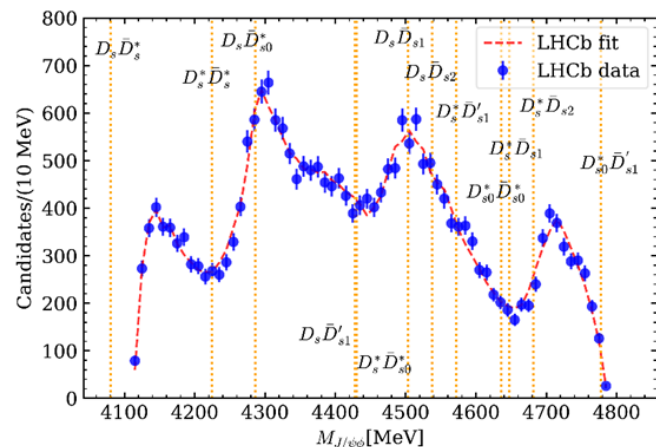


X(3872) and related states



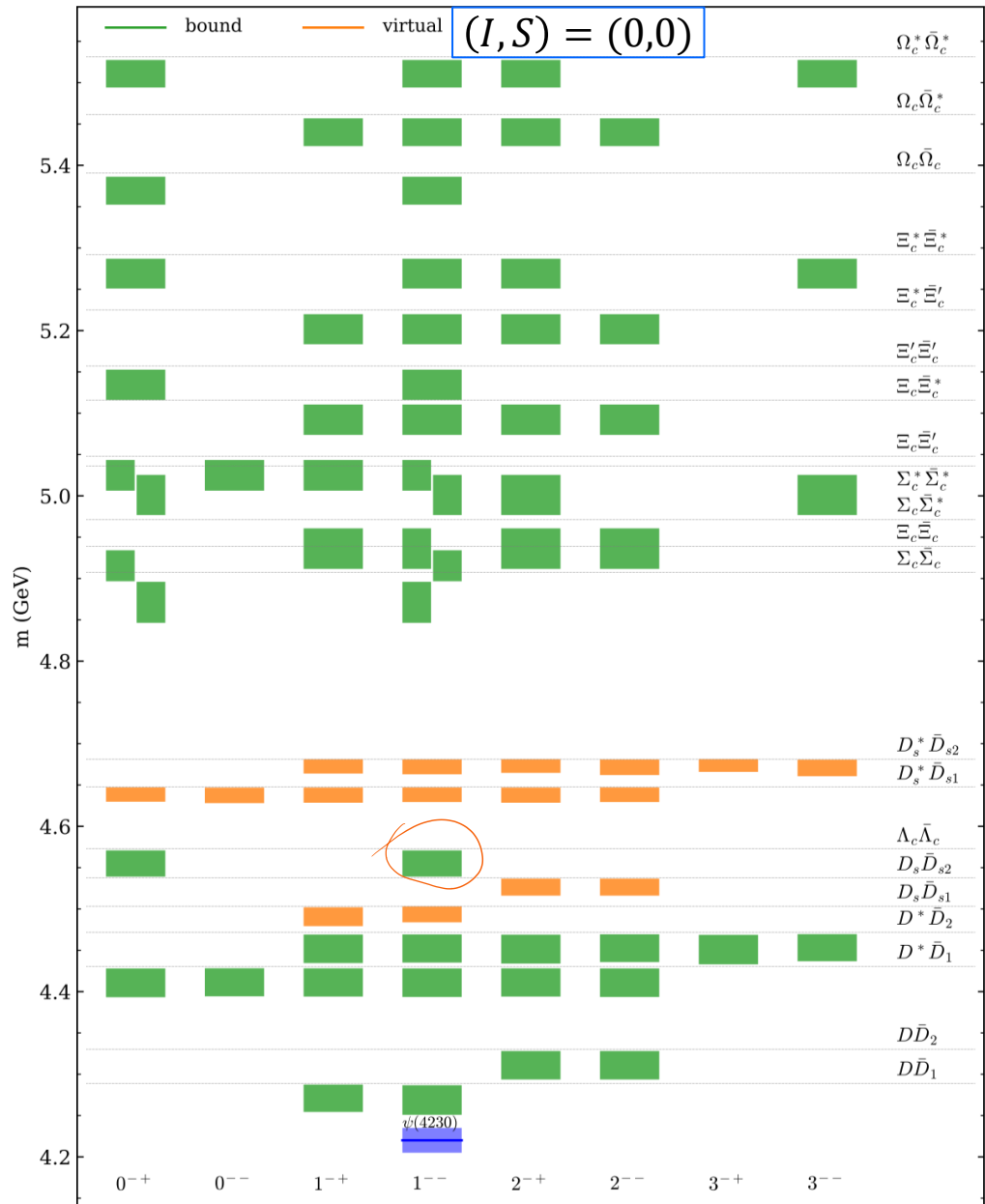
X.-K. Dong, FKG, B.-S. Zou, Progr.Phys. 41 (2021) 65

- ✓ $X(3872)$ as a $\bar{D}D^*$ bound state
- ✓ Negative-C parity partner observed by COMPASS PLB783(2018)334
- ✓ $\bar{D}D$ bound state predicted with lattice Prelovsek et al., JHEP2106,035 and other models e.g., Wong, PRC69, 055202; Zhang et al., PRD74, 014013; Gamermann et al., PRD76, 074016; Nieves et al., PRD86, 056004; ...
- ✓ Evidence for a $D_s^*\bar{D}_s^*$ virtual state in LHCb data?

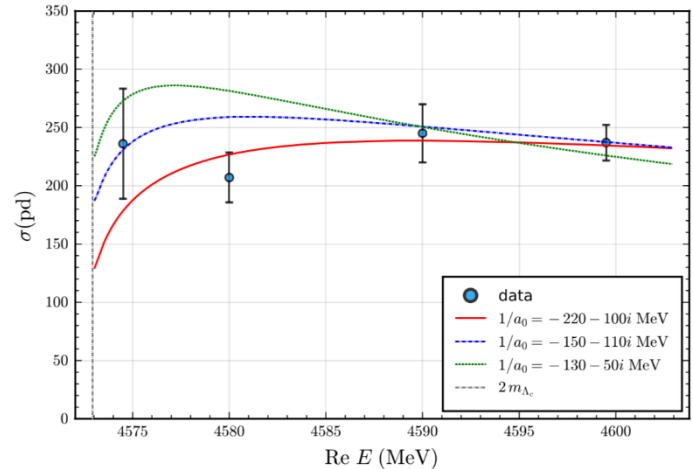


LHCb data: PRL127, 082001

Isoscalar vectors and related states



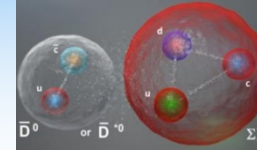
- ✓ $Y(4260)/\psi(4230)$ as a $\bar{D}D_1$ bound state
- ✓ Vector charmonia around 4.4 GeV unclear
- ✓ Evidence for $1^{--} \Lambda_c \bar{\Lambda}_c$ bound state in BESIII data
 - Sommerfeld factor
 - Near-threshold pole
 - Different from $Y(4630/4660)$



Data taken from BESIII, PRL120(2018)132001

- ✓ Many 1^{--} states above 4.8 GeV:
Belle-II, BEPC-II-Upgrade, STCF

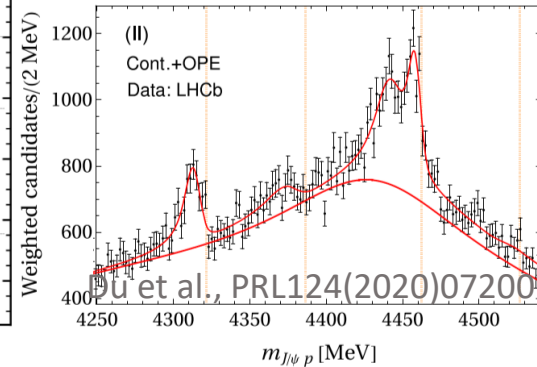
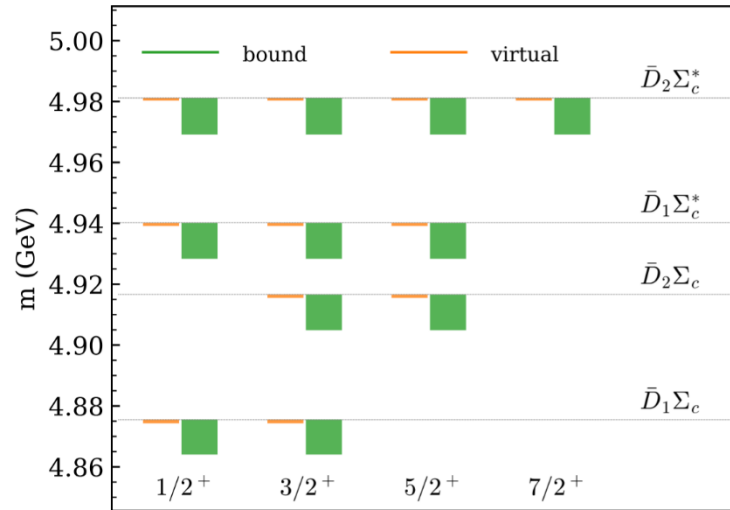
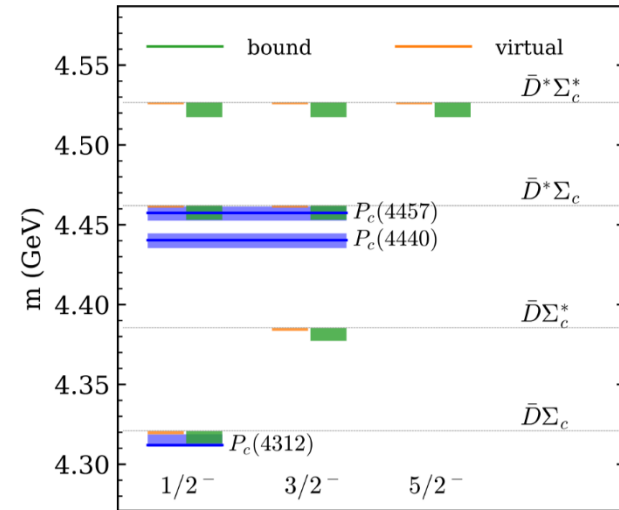
Hidden-charm pentaquarks



$(I, S) = (1/2, 0)$

$(I, S) = (1/2, 0)$

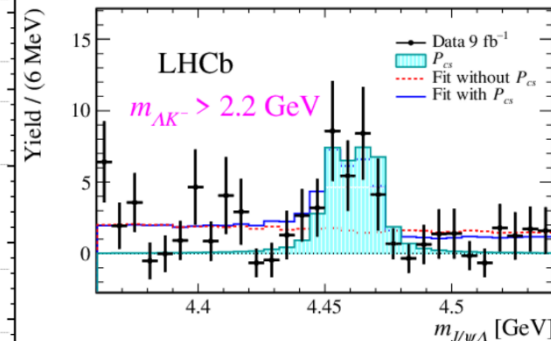
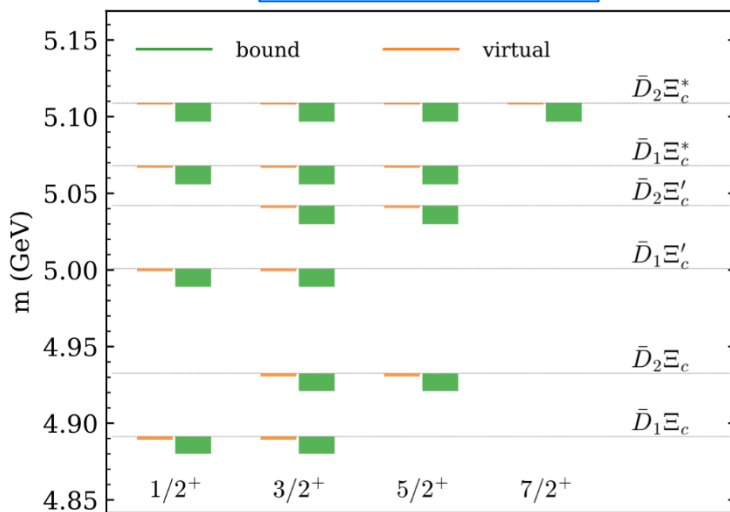
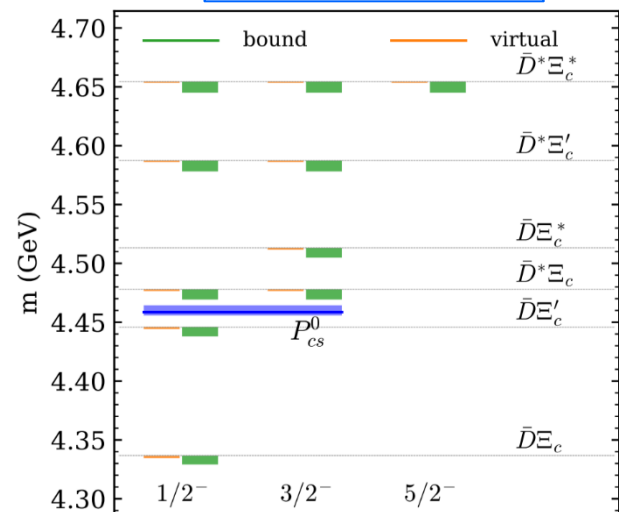
- ✓ The LHCb P_c states as $\bar{D}^{(*)}\Sigma_c$ molecules
- ✓ $\bar{D}\Sigma_c^*$ molecule: hint in the LHCb data



$(I, S) = (0, 1)$

$(I, S) = (0, 1)$

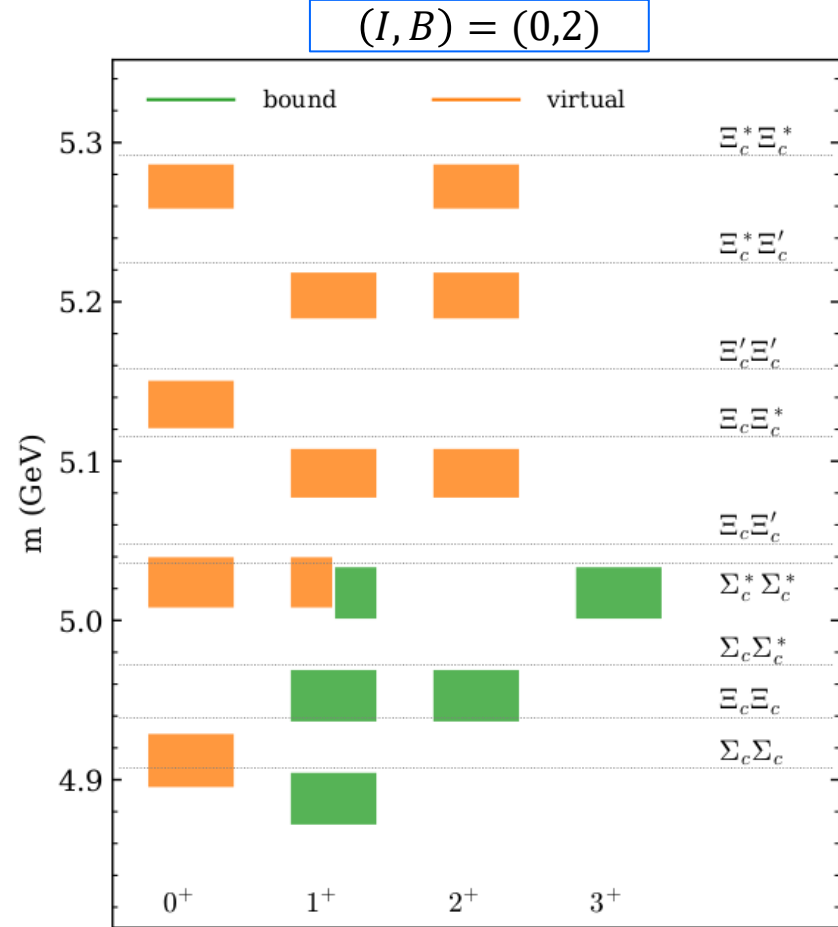
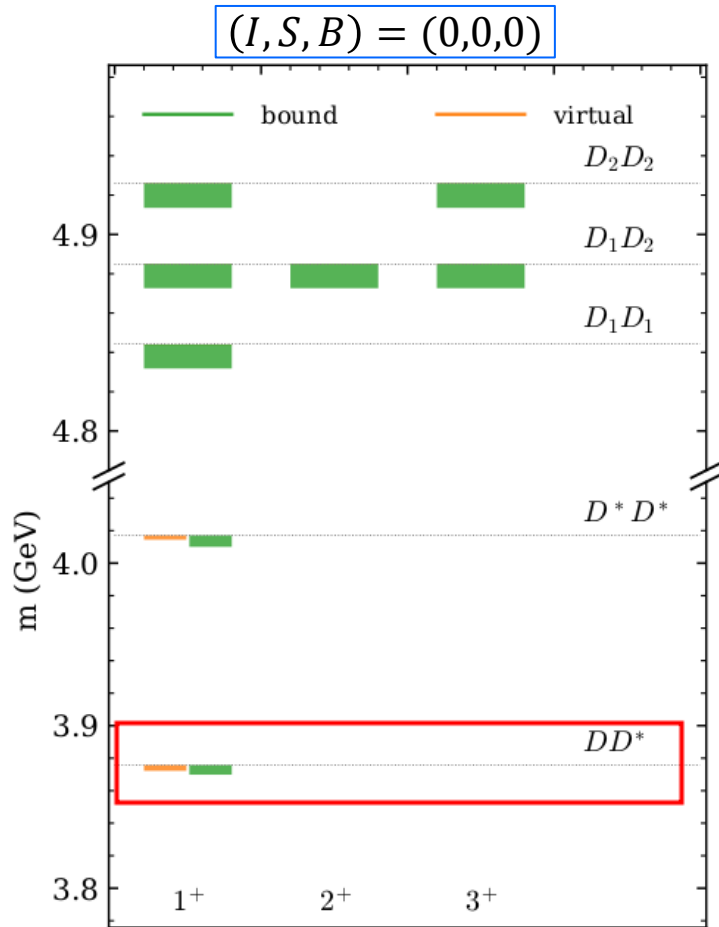
- ✓ The $P_{cs}(4459)$ could be two $\bar{D}^*\Xi_c$ molecules



✓ Many more baryon-antibaryon molecular states above 4.7 GeV

LHCb, Sci.Bull.66,1278

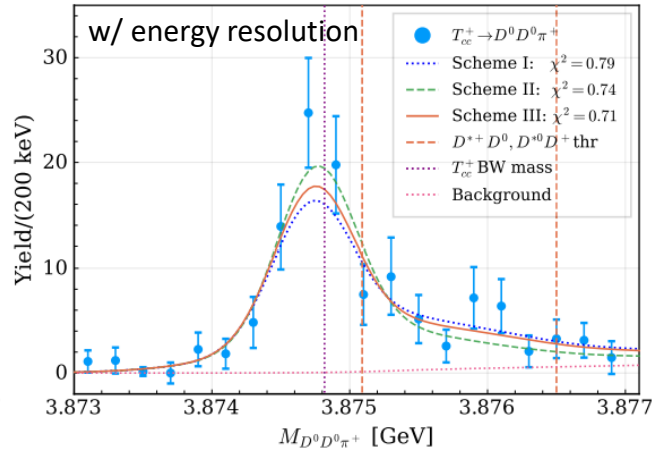
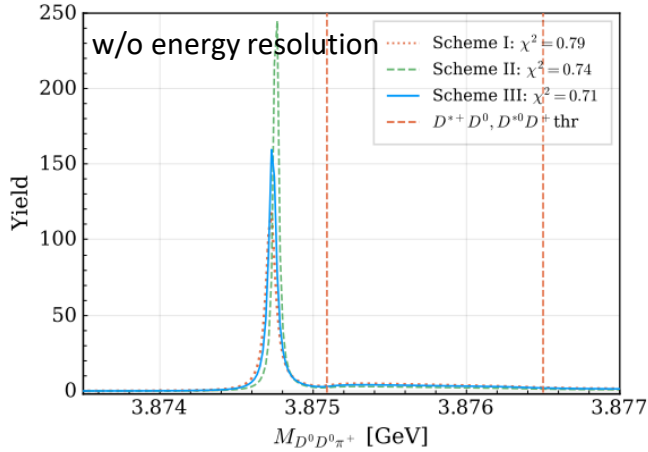
Double-charm



- ✓ There is an isoscalar DD^* molecular state
- ✓ It has a spin partner $1^+ D^* D^*$ state
- ✓ Many other similar double-charm molecular states in other sectors

X.-K. Dong, FKG, B.-S. Zou, CTP73(2021)125201

- Description of the LHCb data in the hadronic molecular picture M.-L. Du et al., arXiv:2110.13765



Isoscalar $D^* D$ molecule, components:

- $D^{*+} D^0 : \sim 73\%$
- $D^{*0} D^+ : \sim 27\%$

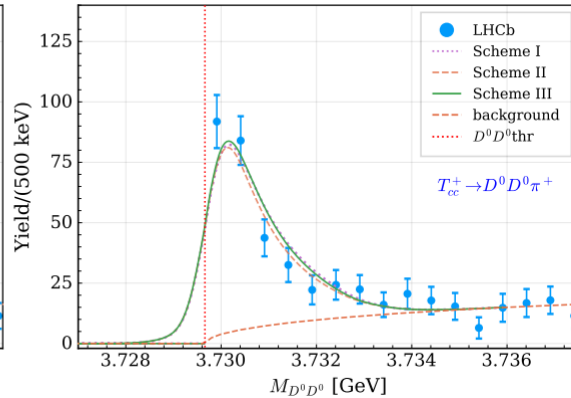
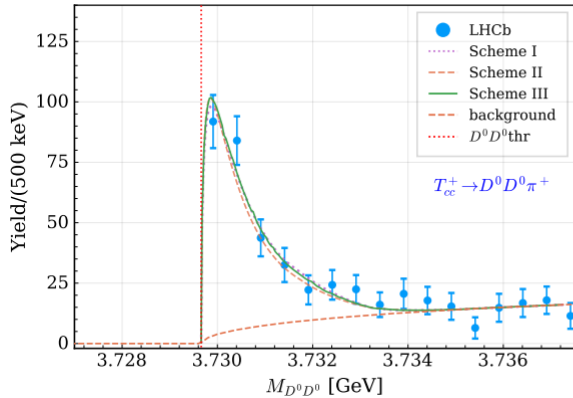
Scheme	I	II	III
Pole [keV]	$-368_{-42}^{+43} - i(37 \pm 0)$ (RS-I)	$-333_{-36}^{+41} - i(18 \pm 1)$ (RS-II)	$-356_{-38}^{+39} - i(28 \pm 1)$ (RS-II)

Contact term + const. Γ_D^*

Contact term + dynamical Γ_D^*

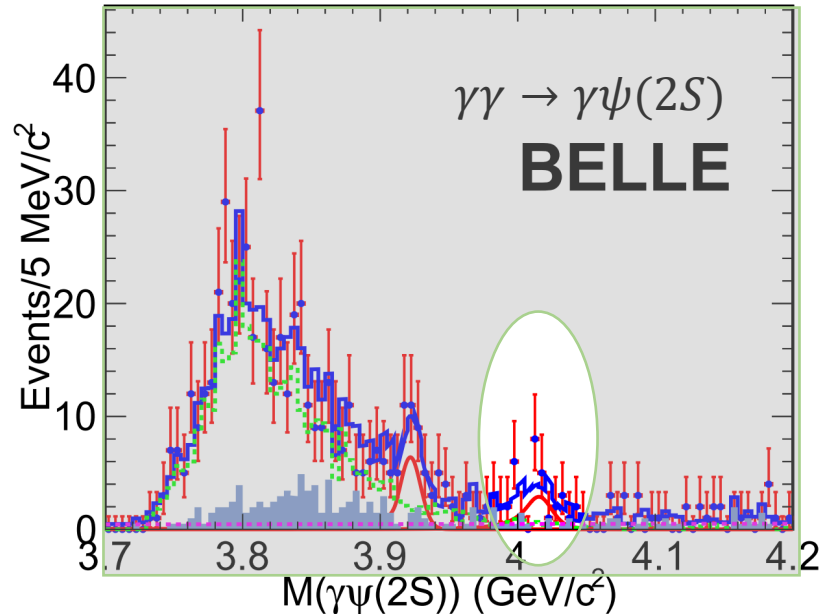
Contact term + OPE + dynamical Γ_D^*

- Predicted DD spectra versus LHCb data



Spin partners

- Structure observed in $\gamma\gamma \rightarrow \gamma\psi(2S)$: evidence for X_2 , the spin partner of $X(3872)$?



$$M = 4014.4 \pm 4.1 \pm 0.5 \text{ MeV},$$

$$\Gamma = 6 \pm 16 \pm 6 \text{ MeV}$$

significance: 3.0σ

Belle, arXiv:2105.06605

- Width of $X_2 \rightarrow D\bar{D}, \bar{D}D^* + c. c.$ predicted in molecular model:

$\sim 2 - 8 \text{ MeV}$ M. Albaladejo, FKG, C. Hidalgo-Duque, J. Nieves, M.P. Valderrama, EPJC75(2015)547

$\sim 50 \text{ MeV}$ V. Baru, E. Epelbaum, A.A. Filin, C. Hanhart, U.-G. Meißner, A.V. Nefediev, PLB763(2016)20

- $1^{+-} D\bar{D}^*$ molecule: $\tilde{X}(3872)$ by COMPASS ?

COMPASS, PLB783(2018)334

- Spin partner of T_{cc}^+ : $T_{cc}^{*+} [D^{*0}D^{*+}]$ with 1^+ , decay modes: $DD\pi, DD\pi\pi, DD\gamma, DD\gamma\gamma$



Conclusion

- General rule for (near-)threshold structures: S-wave attraction, more prominent for heavier particles and stronger attraction
- Strong attraction, then hadronic molecules below threshold, otherwise threshold cusps (and virtual state poles)
- Structures should be **more prominent in bottom than in charm**
- A rich spectrum of hadronic molecules is expected from the VMD model; T_{cc}^+ would have a spin partner with 1^+ around the D^*D^* threshold
- Kinematical singularities (threshold cusp, TS) and resonances are NOT exclusive

Experiments Lattice
EFT, models

Thank you for your attention!

Threshold cusp

- **Unitarity** of the S -matrix: $S S^\dagger = S^\dagger S = \mathbb{1}$, $S_{fi} = \delta_{fi} - i(2\pi)^4 \delta^4(p_f - p_i) T_{fi}$

$$T\text{-matrix: } T_{fi} - T_{fi}^\dagger = -i(2\pi)^4 \underbrace{\sum_n \delta(p_n - p_i) T_{fn}^\dagger T_{ni}}_{\text{all physically accessible states}}$$

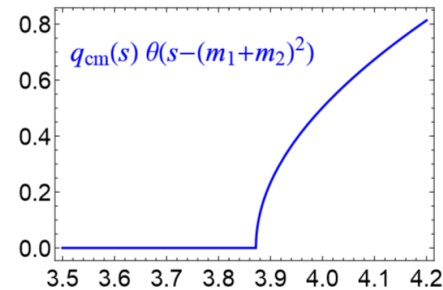
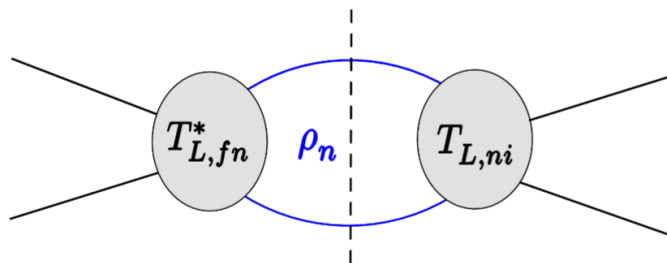
all physically accessible states

assuming all intermediate states are two-body, partial-wave unitarity relation:

$$\text{Im } T_{L,fi}(s) = - \sum_n T_{L,fn}^* \rho_n(s) T_{L,ni}$$

2-body phase space factor: $\rho_n(s) = q_{\text{cm},n}(s)/(2\sqrt{s})\theta(\sqrt{s} - m_{n1} - m_{n2})$,

$$q_{\text{cm},n}(s) = \sqrt{[s - (m_{n1} + m_{n2})^2][s - (m_{n1} - m_{n2})^2]}/(2\sqrt{s})$$

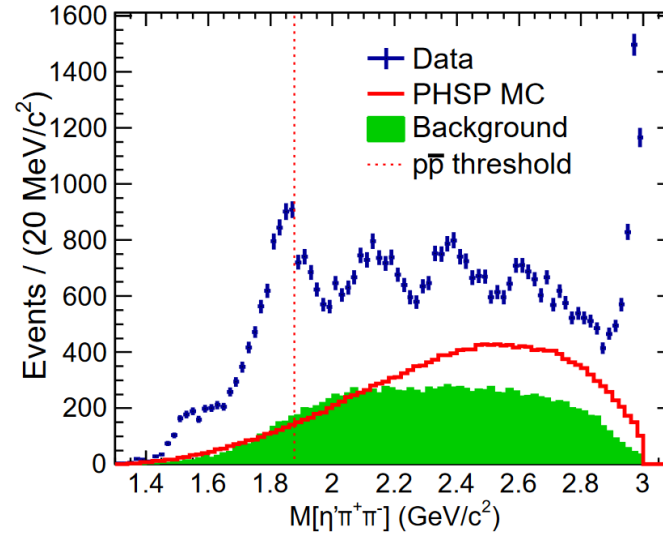
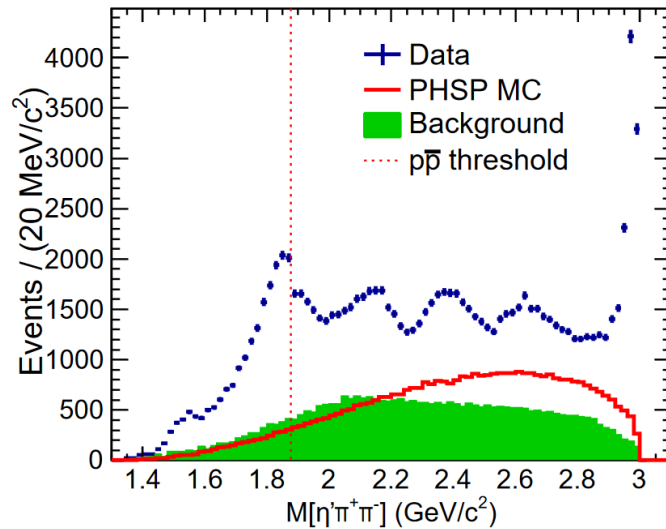


- There is **always** a cusp at an S -wave threshold

Phenomenology

- $p\bar{p}$ threshold in $J/\psi \rightarrow \gamma\eta'\pi^+\pi^-$

BESIII, PRL117(2016)042002



Drastic drop:

- there should be a pole near the $p\bar{p}$ threshold
- $p\bar{p}$ is not the driving channel

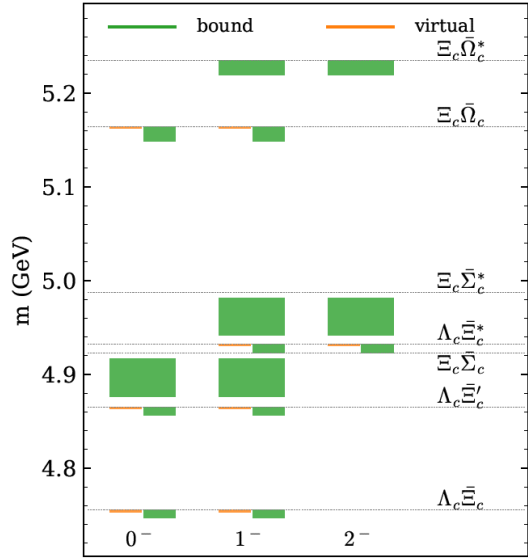
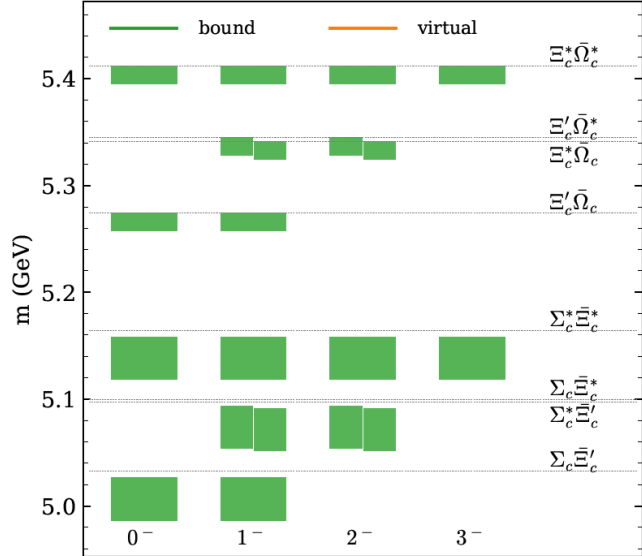
- $D^{(*)}\bar{D}^{(*)}$ should be the driving channels for $X(3872)$, $Z_c(3900)$, $Z_c(4020)$

More states with exotic quantum numbers

$(I, S) = (1, 0)$



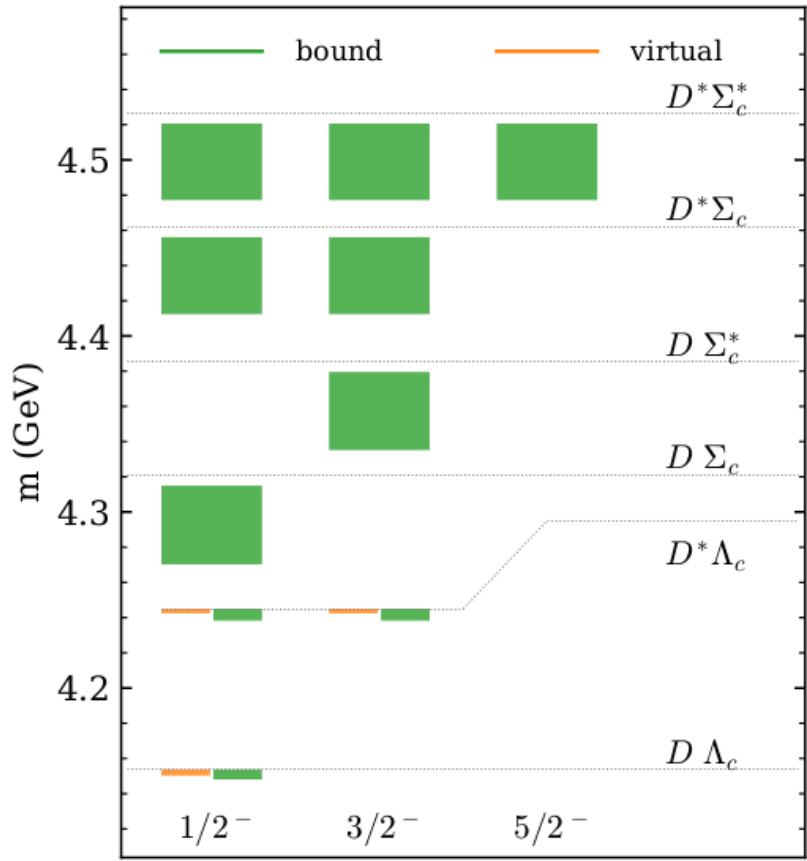
$(I, S) = (1/2, 1)$



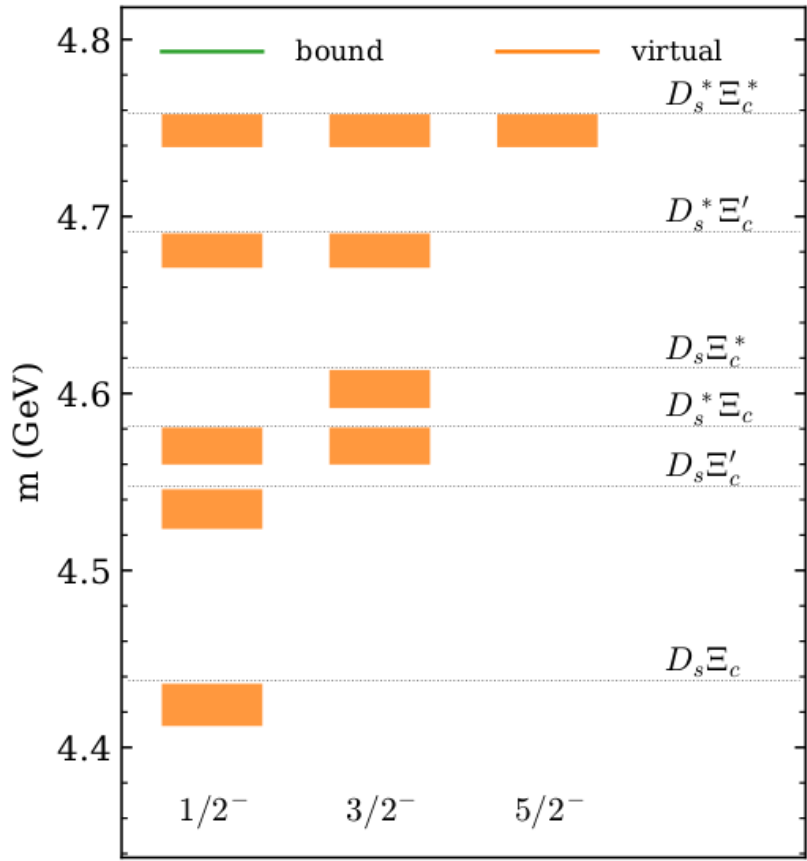
✓ Many baryon-antibaryon molecular states above 4.7 GeV, beyond the current exp. region

Double-charm

$$(I, S, B) = (1/2, -1, 1)$$



$$(I, S, B) = (0, 0, 1)$$

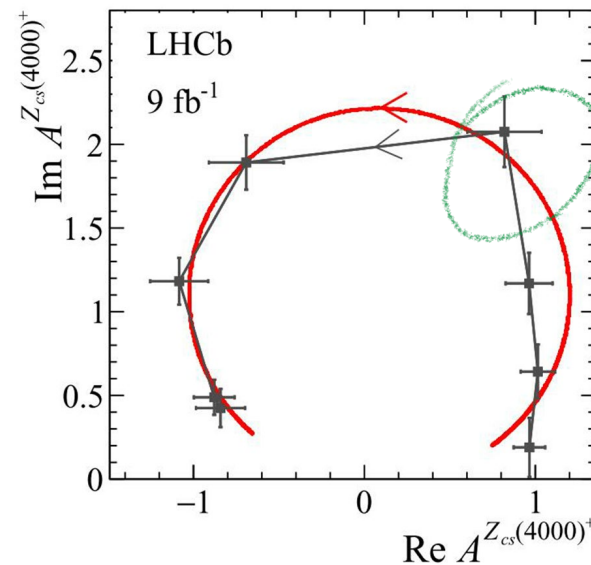
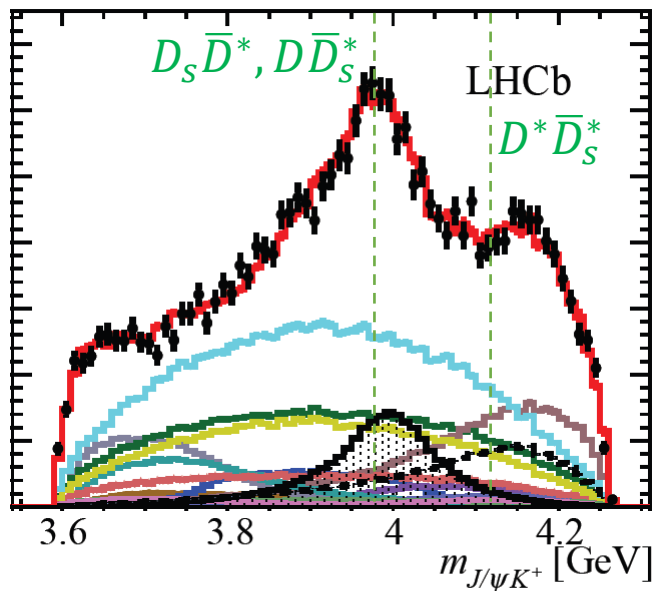


- ✓ The attractions for $D^{(*)} \Sigma_c^{(*)}$ are stronger than those for $\bar{D}^{(*)} \Sigma_c^{(*)}$
- ✓ However, the $D^{(*)} \Sigma_c^{(*)}$ states mix with normal double-charm baryons

X.-K. Dong, FKG, B.-S. Zou, arXiv:2108.02673

Comments on Z_c and Z_{cs}

- ✓ Isovector interaction between $D^{(*)}\bar{D}^{(*)}$ from light vector exchange vanishes
- ✓ Charmonia exchange might be important here: F.Aceti, M.Bayar, E.Oset et al., PRD90(2014)016003
no mass hierarchy, a series of charmonia can be exchanged Dong, FKG, Zou, arXiv:2101.01021
axial-vector meson exchange considered in Yan, Peng, Sanchez Sanchez, Pavon Valderrama 2102.13058
- ✓ $Z_c(3900,4020)$ as $\bar{D}^{(*)}D^*$ virtual states
- ✓ $Z_{cs}(3985)$ as $D_s\bar{D}^*$, DD_s^* virtual state; there should also be a $D^*\bar{D}_s^*$ state around 4.1 GeV
Z. Yang, X. Cao, FKG, J. Nieves, M. Pavon Valderrama, PRD103(2021)074029



LHCb, arXiv: 2103.01803

Comments on Z_c and Z_{cs}

- ✓ Simultaneous fit to the BESIII and LHCb Z_{cs} data: Z_{cs} as virtual states

Ortega, Entem, Fernandez, 2103.07781

